Available online at www.sciencedirect.com
ScienceDirect
ELSEVIER
Dyes and Pigments 76 (2008) 76–81
DYES and PIGMENTS
www.elsevier.com/locate/dyepig

Photocatalytic degradation of dyes over cobalt doped mesoporous SBA-15 under sunlight

Fei Xia [a], Encai Ou [a], Lin Wang [b], Jiaqiang Wang [a,*]

[a] Department of Applied Chemistry, Key Laboratory of Medicinal Chemistry for Natural Resource, Ministry of Education, Yunnan University, 2 Cuihu BeiLu Road, Kunming Yunnan 650091, PR China
[b] Yunnan University of Minority Nationalities, Kunming 650031, PR China

Received 8 August 2006; received in revised form 12 August 2006; accepted 16 August 2006
Available online 6 October 2006

Abstract

Cobalt doped mesoporous silica (Co-SBA-15) was synthesized using templating method and used for the photodegradation of methyl violet and methylthionine chloride under solar light. Co-SBA-15 was characterized by a combination of various physicochemical techniques, such as, N_2 physisorption, diffuse reflectance UV–vis, X-ray diffraction and FT-IR. It was found that Co-SBA-15 in the absence of titania exhibited an obviously photocatalytic efficiency of degradation dyes under solar light irradiation, and its photodegradation rate is comparable with that of Degussa P25. By contrast, undoped SBA-15 exhibited high adsorption capacities but photocatalytically inactive under solar light.

Keywords: Co-SBA-15; Photocatalysis; Adsorption; Degradation of dyes; Methyl violet; Methylthionine chloride

1. Introduction

Various industries such as textiles, paint and varnishes, ink, plastics, pulp and paper and cosmetics use different types of organic dyes and dye intermediates. However, such colored dye effluents pose a major threat to the surrounding ecosystem. Some of the dyes are extremely toxic [1].

Dye effluents can be treated by biological methods, flocculation, reverse osmosis, adsorption on activated charcoal, chemical oxidation methods and advanced oxidation processes [2]. Biological methods have been proved to be ineffective [3–5]. Flocculation, reverse osmosis and adsorption methods transfer the pollutants to other media, thus causing secondary pollution [6,7]. Chemical oxidation methods are not cost effective [8]. Hence there is considerable current interest in developing attractive and more cost-effective methods.

Recent studies have demonstrated that heterogeneous photocatalysis using TiO_2 as photocatalyst appears as the most emerging destructive technology [9]. But, large band gap energy (3.2 eV) for anatase TiO_2 (excitation wavelength <387.5 nm) limits its practical application under the condition of natural solar light [10]. To develop more solar light efficient catalysts, it is very urgent to develop photocatalytic systems which are able to operate effectively under visible light irradiation.

A number of systems have been reported to serve as candidates for this application recently. They include transition-metal doped TiO_2 [11], ZnO [12], nitrogen-doped TiO_2 [13], and the photosensitization degradation of dye pollutants [14,15]. Furthermore, chromium containing mesoporous silica molecular sieves (Cr-HMS) [16] and transition metal (Cr, V, and Fe) based titania loaded MCM-41 materials have tested positive for degradation of organics in visible light. Particularly, the chromium substituted MCM-41 loaded with TiO_2 (TiO_2/Cr–Ti-MCM-41) was found to achieve the highest degradation rates of formic acid and 2,4,6-trichlorophenol [17]. $M/TiO_2/SiO_2$ and M/SiO_2 aerogels with high surface area were also found to be highly active for degradation of gas phase acetaldehyde utilizing visible light [10,18].

---

* Corresponding author. Tel./fax: +86 871 5031567.
E-mail address: jqwang@ynu.edu.cn (J. Wang).

0143-7208/$ - see front matter © 2006 Elsevier Ltd. All rights reserved.
doi:10.1016/j.dyepig.2006.08.008

SBA-15 is a new-style mesoporous silica molecular sieve with uniform hexagonal channels ranging from 5 to 30 nm, thick walls (3.1–6.4 nm), and with higher hydrothermal stability than MCM-41 [19], leading modified SBA-15 widely used in photocatalysis fields. For instance, iron-containing SBA-15 catalyst consisting of crystalline hematite particle oxides supported onto a mesostructured silica matrix has been shown as a promising catalyst for the treatment of phenolic solutions through photo-Fenton processes [20], CdS–ZnSBA-15 was used as photocatalyst for the generation of H_2 from 2-propanol aqueous solution under UV light irradiation [21]. Besides, TiO_2-loaded Cr-modified SBA-15 was prepared for 4-chlorophenol photodegradation under visible light [22]. Moreover, 2,9-dichloroquinacridone sensitized Ti-SBA-15 (DCQ-Ti-SBA-15) was employed to decompose indigo carmine and showed high photocatalytic efficiency under UV light irradiation [23].

However, there is no report on using cobalt doped SBA-15 without loading with titania for the photodegradation of dyes under visible light irradiation so far as we know. The incorporations of Co into the framework of Al-MCM-41 (Co–Al-MCM-41), SiO_2 and TiO_2/SiO_2 aerogels were found to be active for photodegradation of acetaldehyde under visible light irradiation [10,18,24]. Therefore, it was suggested as a good possibility to apply Co ions to dope mesoporous SBA-15 for the first time as a photocatalyst. Herein we report that Co ions incorporated SBA-15 without loading with titania acts as an efficient photocatalyst for the degradation of two organic dyes: methyl violet and methylthionine chloride under solar light.

2. Experimental

2.1. Materials

Two dyes, methyl violet and methylthionine chloride were used without further purification and all of them were of analytical grade. Their molecular formulas, λ_{max} and molecular structures are listed in Table 1.

2.2. Synthesis of photocatalysts

Co-SBA-15 was synthesized with a process modified from Ref. [25]: (1) 0.8 g of triblock copolymer P123 ($EO_{20}PO_{70}EO_{20}$) was dissolved in 25 mL of HCl solution (2 M), followed by the addition of 1.7 g of TEOS. The mixture was stirred at 40 °C for 4 h, and then a requisite amount of Co $(NO_3)_3 \cdot 6H_2O$ was added to the mixture, followed by additional stirring at 40 °C for 20 h. The mixture was then transferred into an autoclave for further condensation at 90 °C for 2 days. (2) After the procedure described above, the pH value of the synthesis system was adjusted up to 7.5 by adding ammonia dropwise at room temperature and the obtained mixture was hydrothermally treated again at 90 °C for another 2 days. The final solid was collected by filtration, washed with water, and dried at room temperature. The surfactants were removed by calcinations at 550 °C for 6 h. For comparison, undoped SBA-15 was also prepared.

2.3. Characterizations

X-ray powder diffraction (XRD) experiments were conducted on a D/max-3B spectrometer with Cu Kα radiation. Scans were made in the 2θ range 0.5–5° with a scan rate of 0.02°/min (low-angle diffraction), and in the 2θ range 7–100° with a scan rate of 10°/min (wide-angle diffraction).

Pore size distributions, BET surface areas, and pore volumes were measured by nitrogen adsorption/desorption using a NOVA 2000e gas sorption analyzer (Quantachrome Corp.). Prior to the analysis, the samples were degassed at 150 °C for 1 h.

UV–vis diffuse reflectance spectra were measured at room temperature in air on a Shimadzu UV-2401PC photometer over the range from 200 to 800 nm.

FT-IR measurements were performed on a Thermo Nicolet AVATAR FT-IR 360 instrument. Potassium bromide pellets containing 0.5% of the catalysts were used in FT-IR experiments and 32 scans were accumulated for each spectrum in transmission, at a spectral resolution of 4 cm^{-1}. The spectrum of dry KBr was taken for background subtraction.

2.4. Photocatalysis studies

The reactions of the photocatalytic decolorization of two dyes (MV and MC) were carried out in a 50 cm^3 glass beaker containing 25 cm^3 of a model solution and 25 mg of

Table 1
Description of dyes

Name of dye	Molecular formulas	λ_{max} (nm)	Molecular structures
MV	$C_{24}H_{28}N_3Cl$	582.0	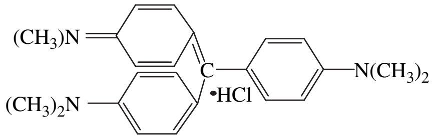
MC	$C_{16}H_{18}ClN_3S$	663.5	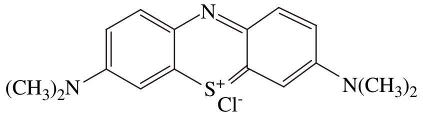

photocatalyst under direct solar light between 10 a.m. and 2 p.m. where the solar intensity fluctuations were minimal. On a sunny day, the solar radiation energy is 16.28–16.50 MJ m^{-2} when there is relatively clear sky in Kunming City, Yunnan Province of China [26]. All of the photocatalysis experiments were carried out on sunny days.

Dye solutions were stirred in the dark for 120 min and care was taken that there was no change in dye concentration due to adsorption before photocatalysis. The control experiments were also conducted under solar light without catalyst to measure any possible direct photolysis of these dyes. Because of the shadowing effect, the optional catalyst loading on the dyes of 1 g dm^{-3} was employed throughout the present study. After the systems reached the adsorption balance, they were exposed for 3 h under solar light. Laboratory film was used to seal the beaker so that the volume of the solutions decreased little after the experiment. The solutions were mixed with a magnetic stirrer during the reaction process. The initial concentration of each solution was equal to 50 mg dm^{-3} with pH 6. Samples were analyzed after centrifugation (1500 rpm for 10 min). The progress of photocatalytic decolorization was measured by vis spectrophotometer (Shanghai Precision 722N).

3. Results and discussion

3.1. Structural analysis of the catalysts

From Fig. 1 it is seen that the low-angle powder X-ray diffraction (XRD) patterns of the sample Co-SBA-15 at 0.5–5° show several diffraction lines in the low 2θ region, clearly indicating that the sample has a regular mesoporous structure which is in good agreement with reported literatures [19,25]. Interestingly, the sample is amorphous and no peaks corresponding to cobalt oxides were observed in the wide-angle diffractograms (Fig. 1, inset). This also indicates that our cobalt oxides were well incorporated into the SBA-15 framework.

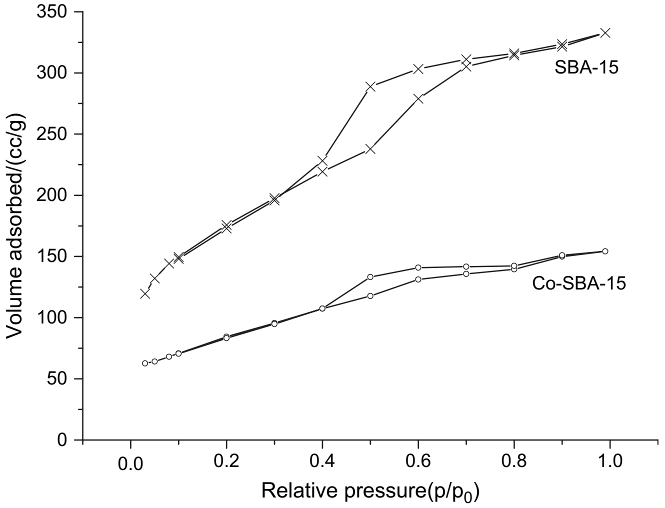

Fig. 2. N_2 adsorption/desorption isotherms of SBA-15 and Co-SBA-15.

Fig. 2 shows the N_2 adsorption/desorption isotherms of SBA-15 and Co-SBA-15. Both samples show typical IV adsorption/desorption isotherms [27]. This result indicates that a large amount of Co was grafted into SBA-15 while retaining a highly ordered mesostructure. The surface area, pore volume, and average pore diameter of Co-SBA-15 (690 m^2/g, 0.51 cc/g, and 32 Å, respectively) were found to be slightly decreased compared with those of SBA-15 (701 m^2/g, 0.64 cc/g, and 45 Å, respectively). The slight decrease of these textural properties could be due to a coalescence process since sintering is favored by the presence of dopants [28].

Fig. 3 presents FT-IR spectra of calcined SBA-15 and Co-SBA-15 between 400 and 4000 cm^{-1}. The broad band from 3400 to 3700 cm^{-1} is assigned to stretching frequencies of hydrogen bound silanols. In the hydroxyl region (3000–4000 cm^{-1}), the broad band is both observed at ca. 3420 cm^{-1} for SBA-15, and Co-SBA-15 [29]. The three peaks at 470 cm^{-1}, 799 cm^{-1}, and 1090 cm^{-1} corresponded to

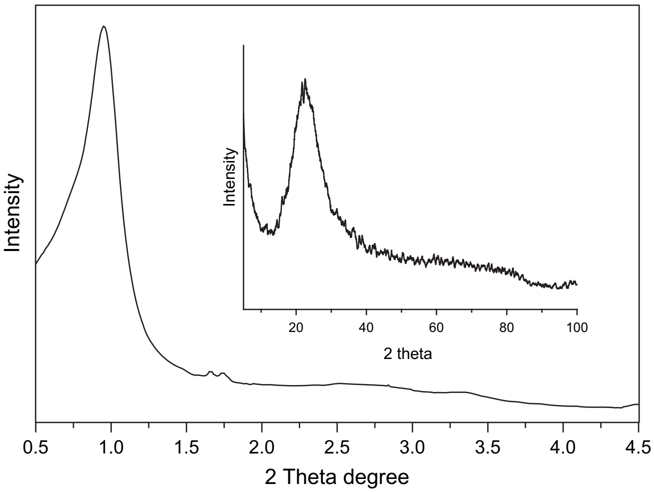

Fig. 1. XRD patterns of Co-SBA-15.

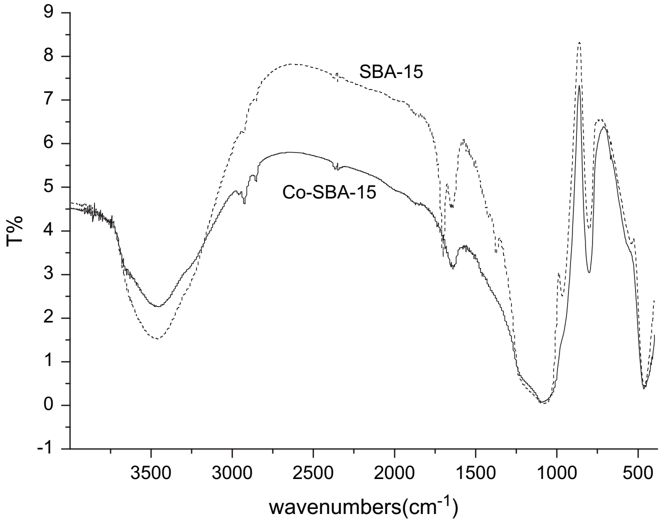

Fig. 3. FT-IR spectra of SBA-15 and Co-SBA-15.

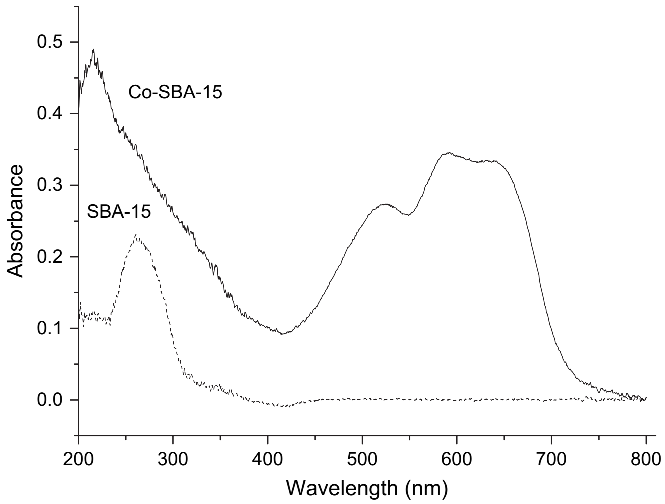

Fig. 4. UV–vis absorption spectra of SBA-15 and Co-SBA-15.

rocking, bending (or symmetric stretching), and asymmetric stretching of the intertetrahedral oxygen atoms in the SiO_2 structure, respectively, for the IR patterns of calcined SBA-15 [31,32]. The peak at 970 cm^{-1} (shoulder) reveals a characteristic vibration which corresponds to the stretching of nonbridging oxygen atoms ($Si–O^{\delta-}$) of an Si–OH stretch [31]. With the incorporation of cobalt into the framework of SBA-15, the absorbance intensities of 960 cm^{-1} decreased, implying that Si–OH groups were consumed and transformed to Si–O–Co bonds. Meanwhile, inflated inclinations were shown in 920–940 cm^{-1}, showing the combination bands of Co–O fundamental vibrational modes [32]. The surface hydroxyl groups have been recognized to play an important role in the photodegradation process through their interactions with photogenerated holes [30].

The diffuse reflectance UV–vis spectra of SBA-15 and Co-SBA-15 are given in Fig. 4. Cobalt incorporation increased the absorption in both visible and UV range compared with undoped SBA-15. It is also seen that Co-SBA-15 exhibited three distinct absorption bands around 215, 525 and 592 nm which may be due to charge transfer from O^{2-} to Co^{3+} [18]. Moreover, the Co-SBA-15 sample showed increased absorption over a broad range of 400–700 nm compared with undoped SBA-15, thus justifying why it can be a potentially good candidate for performing photochemical reactions under solar light.

3.2. Evaluation of photocatalytic activity

After reaching adsorption balance (120 min in the dark), the variations for the concentrations of the studied dyes are summarized in Table 2. It is clear that both SBA-15 and Co-SBA-15 have very strong adsorptions for these two dyes and undoped SBA-15 exhibited much higher adsorption capacity than Co-SBA-15.

The effects of direct photolysis of dyes without photocatalyst are also listed in Table 2. It is seen that the degradation rates of MV and MC in the absence of photocatalyst are less than 4%. However, in order to obtain the real photodegradation rate due to the photocatalysis in the presence of photocatalysts, the decreases of the dye concentration because of the adsorption and direct photolysis should be deducted. The decrease due to adsorption can be deducted after the adsorption equilibrium was achieved. Therefore, photodegradation rate is defined as:

Table 2
Direct photolysis rate, adsorption rate, and photodegradation rate of the photocatalytic experiments (dye solutions: 25 mL, 50 mg dm^{-3})

Name of dye	Catalysts	Direct photolysis rate (%)	Adsorption rate (%)	Photodegradation rate (%)
MV	SBA-15	1	89	7
	Co-SBA-15		82	69
MC	SBA-15	4	94	6
	Co-SBA-15		79	76

$$\text{photodegradation rate} = \frac{(C_0 - C_a - C_b)}{C_0} 100.$$

C_0 is the initial concentration, C_a is the concentration after photodegradation under solar light, and C_b is the decreased concentration because of direct photolysis.

Based on the above definition, the photodegradation rates using SBA-15 and Co-SBA-15 as photocatalysts are calculated and included in Table 2. Blank experiments indicate that the direct photolysis of MV is negligible when illuminated with solar light in the absence of catalysts. So, MV was used to evaluate the photocatalytic activity of Co-SBA-15. Fig. 5 shows the photodegradation profile of MV with 50 mg dm^{-3} aqueous solution loaded of 1 g dm^{-3} catalyst. The photodegradation rate of Co-SBA-15 was compared with those of SBA-15 and Degussa P25. Within 150 min of solar light irradiation, photodegradation rates of MV over SBA-15, Co-SBA-15, and P25 are 5, 61, and 63%, respectively. It is obvious that without doping cobalt, SBA-15 exhibited negligible photoactivity,

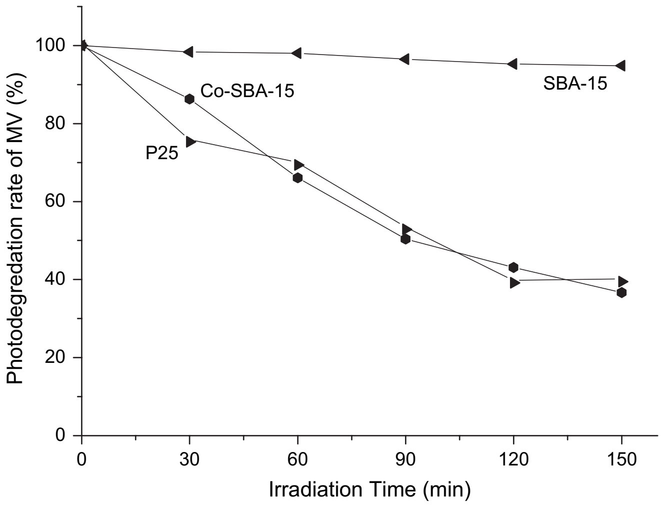

Fig. 5. Comparison of photodegradation rates of MV over Ce/FSM-16, FSM-16 and Degussa P25 under solar light.

whereas doping cobalt resulted in a significant increase of the photoactivity of Co-SBA-15 which is even comparable with Degussa P25 under solar light.

It was also observed that undoped SBA-15 did not exhibit significant activity for MC. By contrast, Co-SBA-15 exhibited significant photodegradation rates (76%).

3.3. Photodegradation mechanisms

The above results indicate that Co-SBA-15 exhibited very good photoactivity under solar light, and undoped SBA-15 had no significant photoactivity but with significant adsorption capacities for these dyes. Visible light activity of Co-SBA-15 samples can be attributed to some extent to the formation of higher oxidation states of Co upon calcination at 550 °C. Co sample changed from pale blue grey to darker blue grey (Co^{3+}). Moreover, the incorporation of cobalt significantly increased the absorption both in visible and UV range compared with undoped SBA-15 which might account for the increased efficiency of the catalyst under sunlight and UV irradiation. The photoactivity probably arises due to the presence of Co^{2+}/Co^{3+} redox couple in the catalyst. Thus, these results indicate that SBA-15 can serve as a support for well dispersed transition metal ions that behave as efficient visible and UV light photocatalysts for the photodegradation of dyes.

4. Conclusions

This study mainly reports solar light induced photodegradation of dyes by cobalt doped SBA-15 and the powerful adsorption capacity of SBA-15. Of particular interest for the work reported here are several things: (1) Co doped SBA-15 was successfully synthesized via templating method, and the solar photodegradation rates of two organic dyes (methyl violet and methylthionine chloride) are comparable with that of Degussa P25. (2) Co-SBA-15 shows an enhanced photocatalytic efficiency of degradation dyes than SBA-15 under solar light irradiation.

Acknowledgements

The authors thank the National Natural Science Foundation of China (Project 20463003) and Natural Science Foundation of Yunnan Province (Project 2004E0003Z, 2003E0007R and 2003E0004Q) for financial support. We also thank Center for Advanced Studies of Medicinal and Organic Chemistry, Yunnan University for partial financial support.

References

[1] Arslan J, Balcioglu IA, Bahnemann DW. Advanced chemical oxidation of reactive dyes in simulated dyehouse effluents by ferrioxalate-Fenton/UV-A and TiO_2/UV-A processes. Dyes and Pigments 2000;47(3):207–9.

[2] Slokar YM, Le Marechal AM. Methods of decoloration of textile wastewaters. Dyes and Pigments 1998;37(4):335–56.

[3] Hu C, Yu JC, Huo Z, Wong PK. Effects of acidity and inorganic ions on the photocatalytic degradation of different azo dyes. Applied Catalysis B: Environmental 2003;46(1):35–47.

[4] Wang Y. Solar photocatalytic degradation of eight commercial dyes in TiO_2. Water Research 2000;34(3):990–4.

[5] Pearce CI, Lloyd JR, Guthrie JT. The removal of color from textile wastewater using whole bacterial cells: a review. Dyes and Pigments 2003;58(3):179–96.

[6] Tanaka K, Padermpole K, Hisanaga T. Photocatalytic degradation of commercial azo dyes. Water Research 2000;34(1):327–33.

[7] Sahoo C, Gupta AK, Anjali P. Photocatalytic degradation of Crystal Violet (C.I. Basic Violet 3) on silver ion doped TiO_2. Dyes and Pigments 2005;66(2):189–96.

[8] Baban A, Yedilar A, Lienert D, Kemerder N, Kettrup A. Ozonation of high strength segregated effluents from a woolen textile dyeing and finishing plant. Dyes and Pigments 2003;58(2):93–8.

[9] Konstantinou IK, Albanis TA. TiO_2-assisted photocatalytic degradation of azo dyes in aqueous solution: kinetic and mechanistic investigations: a review. Applied Catalysis B: Environmental 2004;49(1):1–14.

[10] Wang J, Uma S, Klabunde KJ. Visible light photocatalysis in transition metal incorporated titania–silica aerogels. Applied Catalysis B: Environmental 2004;48(2):151–4.

[11] Nagaveni K, Sivalingam G, Hegde MS, Madras G. Report on the microsymposium air pollution abatement. Applied Catalysis B: Environmental 2004;48(1):83–93.

[12] Sakthivela S, Neppolianb B, Shankarb MV, Arabindoob B, Palanichamyb M, Murugesanb V. Solar photocatalytic degradation of azo dye: comparison of photocatalytic efficiency of ZnO and TiO_2. Solar Energy Materials and Solar Cells 2003;77:65–82.

[13] Asahi R, Morikawa T, Ohwaki T, Aoki K, Taga Y. Visible light photocatalysis in nitrogen-doped titanium oxides. Science 2001;293:269–71.

[14] Chen C, Li X, Ma W, Zhao J, Hidaka H, Serpone N. Effect of transition metal ions on the TiO_2-assisted photodegradation of dyes under visible irradiation: a probe for the interfacial electron transfer process and reaction mechanism. The Journal of Physical Chemistry B 2002;106(2):318–24.

[15] Ji H, Ma W, Huang Y, Zhao J, Wang Z. The review on the photocatalysis of visible induced TiO_2. Chinese Science Bulletin 2003;48:2199–203.

[16] Yamashita H, Katsuhiro Y, Ariyuki M, Higshimoto S, Che M, Anpo M. Photocatalytic reactions on chromium containing mesoporous silica molecular sieves (Cr-HMS) under visible light irradiation: decomposition of NO and partial oxidation of propane. Chemical Communications 2001;1(5):435–6.

[17] Davydov L, Reddy P, France P, Smirniortis PG. Transition-metal-substituted titania-loaded MCM-41 as photocatalysts for the degradation of aqueous organics in visible light. Journal of Catalysis 2001;203(1):157–67.

[18] Wang J, Uma S, Klabunde KJ. Visible light photocatalytic activities of transition metal oxide/silica aerogels. Microporous and Mesoporous Materials 2004;75:143–7.

[19] Zhao D, Huo Q, Feng J, Chmelka BF, Stucky GD. Nonionic triblock and star diblock copolymer and oligomeric surfactant syntheses of highly ordered, hydrothermally stable, mesoporous silica structures. Journal of the American Chemical Society 1998;120(24):6024–36.

[20] Martinez F, Calleja G, Melero JA, Molina R. Heterogeneous photo-Fenton degradation of phenolic aqueous solutions over iron-containing SBA-15 catalyst. Applied Catalysis B: Environmental 2005;60(3):181–90.

[21] Takayuki H, Masanori N, Komasawa I. Structural characteristics of modified activated carbons and adsorption of explosives. Journal of Colloid and Interface Science 2003;268(2):388–99.

[22] Sun B, Reddy EP, Smirniotis PG. TiO_2-loaded Cr-modified molecular sieves for 4-chlorophenol photodegradation under visible light. Journal of Catalysis 2006;237(2):388–99.

[23] Ding HM, Sun H, Shan YK. Preparation and characterization of mesoporous SBA-15 supported dye-sensitized TiO_2 photocatalyst. Journal of Photochemistry and Photobiology A: Chemistry 2005;169(1):101–7.

[24] Rodrigues S, Uma S, Martyanov IN, Klabunde KJ. Visible light induced photocatalytic activity for degradation of acetaldehyde using transition metal incorporated Al-MCM-41 (aluminum doped silica zeolitic material).

Journal of Photochemistry and Photobiology A: Chemistry 2004; 165(1):51–8.

[25] Wu S, Han Y, Zou YC, Song JW, Zhao L, Di Y, et al. Synthesis of heteroatom substituted SBA-15 by the "pH-adjusting" method. Chemistry of Materials 2004;16(3):486–92.

[26] Li M, Huang HB, Wang RZ, Wang LL, Yang WM, Cai WD. Study on intermittent refrigeration phenomenon for solar solid adsorption refrigeration. Applied Thermal Engineering 2005;25(11):1614–22.

[27] Zhao D, Feng J, Huo Q, Melosh N, Fredrickson GH, Chmelka BF, et al. Triblock copolymer syntheses of mesoporous silica with periodic 50. Science 1998;279:548.

[28] Paola AD, Palmisano L, Schiavello M, Uosaki K, Ikeda S, Ohtani B. Preparation of polycrystalline TiO_2 photocatalysts impregnated with various transition metal ions: characterization and photocatalytic activity for the degradation of 4-nitrophenol. The Journal of Physical Chemistry B 2002;106(3):637–45.

[29] Laha SC, Mukherjee P, Sainkar SR, Kumar R. Cerium containing MCM-41-type mesoporous materials and their acidic and redox catalytic properties. Journal of Catalysis 2002;207(2):213–23.

[30] Xie Y, Yuan C. Visible-light responsive cerium ion modified titania sol and nanocrystallites for X-3B dye photodegradation. Applied Catalysis B: Environmental 2003;46(2):251–9.

[31] Primeau M, Vautey C, Langlet M. The effect of thermal annealing on aerosol–gel deposited SiO_2 films: a FTIR deconvolution study. Thin Solid Films 1997;310(1):47–56.

[32] Klingenberg B, Vannice MA. Influence of pretreatment on lanthanum nitrate, carbonate, and oxide powders. Chemistry of Materials 1996;8(12):2755–68.